

IMPULSE RADIATING ANTENNAS

Carl E. Baum
Phillips Laboratory
Kirtland AFB, NM 87117

Everett G. Farr
Farr Research
Albuquerque, NM 87123

ABSTRACT

A number of applications require radiation of a short pulse of electromagnetic energy out to large distances. These applications include target discrimination in a cluttered environment (e.g., looking over the ocean), aircraft identification by taking a "TDR" of its major scattering centers, and target location through foliage. The Impulse Radiating Antenna (IRA) has generated widespread interest for its ability to radiate a broadband pulse. The purpose of this paper is to summarize recent work on Impulse Radiating Antennas.

INTRODUCTION

Impulse Radiating Antennas (IRAs) are meant to satisfy the need for a radiating device for one class of transient radars. This class of radar attempts to solve several problems, such as target identification by scattering centers on aircraft, target discrimination in a highly cluttered environment such as when looking over the ocean, and foliage penetration. We provide here the basic theory of Impulse Radiating Antennas, and apply that theory to some practical examples.

BASIC THEORY

Impulse radiating antennas consist of a conical TEM feed that attaches to a reflector antenna. The load at the attachment point is chosen so that at low frequencies the antenna behaves as a $p \times m$ dipole with a cardioid radiation pattern^{1,2}. An example of an IRA is shown in Figure 1.

Before providing specific designs for IRA's, we first describe a simple theory on which the devices are based. Consider a planar aperture as shown in Figure 2, whose tangential electric field is described by³

$$\tilde{E}_t(r, s) = e^{-\gamma \hat{l}_o \cdot r'} E_o \tilde{f}(s) g(r') \quad (2.1)$$

where the usual convention of primed coordinates referring to the source and unprimed coordinates referring to the observation point has been used. This is just a plane-wave distribution with a uniform time dependence of $f(t)$ in the time domain. The spatial distribution in the aperture is handled by $g(\hat{r}')$, and the direction of maximum radiation is \hat{l}_o . It is shown by Baum³ that the radiated field is just

$$\tilde{E}_f(r, s) = e^{-\gamma r} \frac{E_o A}{2\pi r c} s \tilde{f}(s) \tilde{F}_a(\hat{l}_r, s) \quad (2.2)$$

where the aperture function is

$$\tilde{F}_a(\hat{l}_r, s) = \frac{1}{A} \left[(\hat{l}_z \cdot \hat{l}_r) 1 - \hat{l}_z \hat{l}_r \right] \cdot \int_S e^{\gamma [\hat{l}_r - \hat{l}_o] \cdot r'} \tilde{g}(\hat{r}') dS' \quad (2.3)$$

and the following definitions apply

$$\begin{aligned}
A &= \text{Aperture area}, & 1 &= \bar{1}_x \bar{1}_x + \bar{1}_y \bar{1}_y + \bar{1}_z \bar{1}_z \\
1_z &= \bar{1}_x \bar{1}_x + \bar{1}_y \bar{1}_y, & 1_r &= 1 - \bar{1}_r \bar{1}_r
\end{aligned}
\tag{2.4}$$

If we now specialize the above equations to a uniform plane wave in the aperture, then

$$g(r') = \begin{cases} 1_y & \text{on } S \\ 0 & \text{off } S \end{cases}
\tag{2.5}$$

Furthermore, if we specify that the observation point is on boresight ($1_r = 1_o$), then the above equations simplify considerably to

$$\tilde{F}_a(1_r, s) = 1_y, \quad \tilde{E}_f(r, s) = e^{-\gamma r} \frac{E_o A}{2\pi r c} s f(s) 1_y
\tag{2.6}$$

Thus, if the aperture field has a step-function time dependence, then the radiated field on boresight is

$$\tilde{E}_f(r, t) = \frac{E_o A}{2\pi r c} \delta(t - r/c) 1_y
\tag{2.7}$$

This delta function requires some interpretation.

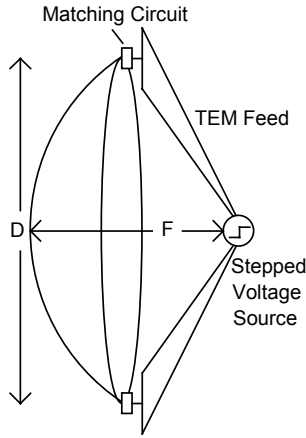


Figure 1. An IRA.

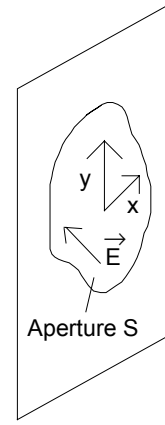


Figure 2. The aperture field.

The problem we face is that on boresight, the energy density is infinite, for bounded aperture fields. Since this is clearly nonphysical, greater care must be taken with the aperture integral in the boresight direction. It has been shown that a more careful aperture field integration leads to³

$$E(z1_z) = 1_z E_o u(t - z/c), \quad 0 < t - z/c < \Delta t
\tag{2.8}$$

where Δt is the clear time required to first see the edge of the aperture. The above is a step function lasting for a time Δt . For a circular aperture of radius a , $\Delta t \approx a^2/(2rc)$, so the integral of the electric field for the duration of this step function is just

$$\int E(z1_z, t) dt = 1_y \frac{E_o a^2}{2rc}
\tag{2.9}$$

This provides the same integral as that generated by integrating the delta function of (2.7).

In order to account for the unusual behavior on boresight, we define an approximate delta function $\delta_a(r, t)$, which has the following properties. Its area is unity, its peak magnitude is proportional to r , and its width is proportional to $1/r$. As $r \rightarrow \infty$, this becomes a true delta function, and $\delta_a(r, t)/r$ has a peak which is constant with r . Thus, $\delta_a(r, t)$ should be used instead of $\delta(t)$ where required to maintain finite energy.

The Aperture-Field Integral

The integral of the aperture field was carried out in the previous section for the trivial case of a circular aperture excited uniformly with a step function. In this section we generalize the above results for more arbitrary aperture distributions. These results will provide an effective height that characterizes the radiation on boresight for an aperture.

Consider an aperture field generated by the transmission line formed by two parallel wires. A diagram of this is shown in Figure 3. As we saw in the previous section, the radiated electric field on boresight is

$$E_f(r, t) = \frac{\delta_a(t)}{2\pi cr} \int_{S_a} E_t(x, y) dS' \quad (3.1)$$

where $\delta_a(t)$ is the approximate Dirac delta function as described in the previous section. The integral can be carried out for several geometries using contour integration in the complex plane. Consider the aperture distribution generated by two parallel wires as shown in Figure 3. If there is a voltage V between the two conductors, and the two conductors form a transmission line of characteristic impedance $f_g Z_o$, then let us define an aperture height such that⁴

$$\frac{V}{f_g} h_a = \int_{S_a} E_t(x, y) dS', \quad Z_o = \sqrt{\mu_o / \epsilon_o} \quad (3.2)$$

This provides a simple way of expressing the far field

$$E_f(r, t) = \frac{V}{2\pi c f_g r} h_a \delta_a(t) \quad (3.3)$$

One now needs to perform the integration in (3.2) in order to find the aperture height.

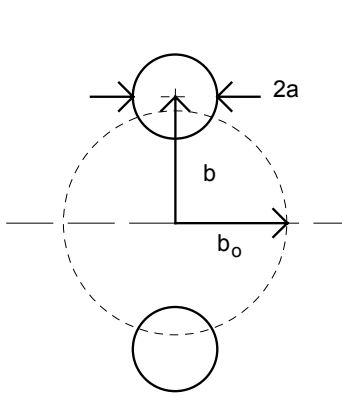


Figure 3. Transmission line for forming the aperture field.

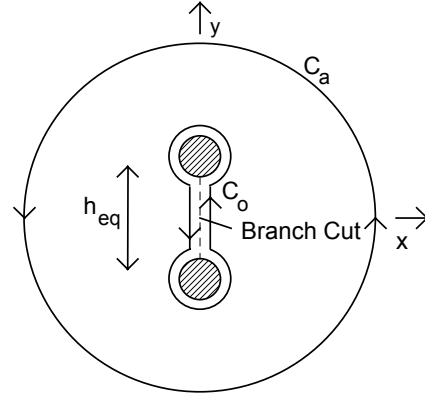


Figure 4. The contour to be integrated.

In order to perform the integration, we convert the vector electric field to a single complex function in the complex plane (Figure 4). The aperture electric field can be expressed as the two-dimensional gradient of a complex potential function. Thus,

$$\begin{aligned} \zeta = x - jy &\equiv \text{complex coordinate} \quad , & w(\zeta) = u(\zeta) - jv(\zeta) &\equiv \text{complex potential} \\ f_g = \Delta u / \Delta v & \quad , & E(\zeta) = E_x(\zeta) - jE_y(\zeta) &= -\frac{V}{\Delta u} \frac{dw(\zeta)}{d\zeta} \end{aligned} \quad (3.4)$$

We now cast the integral into a complex surface integral as follows

$$\Upsilon = \Upsilon_x l_x + \Upsilon_y l_y = \int_{S_a} E(x, y) dS' \quad (3.5)$$

$$\Upsilon = \Upsilon_x - j\Upsilon_y = \int_{S_a} E(\zeta) dS' = -\frac{V}{\Delta u} \int_{S_a} \frac{dw(\zeta)}{d\zeta} dS' \quad (3.6)$$

By Green's theorem, the surface integral of a complex function can be recast as a contour integral⁴, so

$$\begin{aligned}
h_a &= h_{a_x}(\zeta) - j h_{a_y}(\zeta) = \frac{f_g}{V} \Upsilon = \frac{1}{\Delta v} \int_{S_a} \frac{dw(\zeta)}{d\zeta} dS' = \frac{j}{2\Delta v} \oint_{C_a} w d\zeta^* \\
&= \frac{j}{\Delta v} \oint_{C_a} u d\zeta^* = -\frac{j}{\Delta v} \oint_{C_a} v d\zeta^*
\end{aligned} \tag{3.7}$$

Note the branch cut in Figure 4 which makes v (the magnetic potential) single-valued. Therefore, the contribution from C_o is strictly subtracted, but gives zero in some of the above formulas. We now have a simple form for calculating the effective height of an antenna. For the two-wire problem, the complex potential function is obtained from a standard text such as Smythe⁵, so

$$w(\zeta) = 2j \operatorname{arccot}(\zeta/a) \tag{3.8}$$

This can be substituted into (3.7) for various aperture shapes, so effective heights can be determined simply. If the feed wires are thin, we find the aperture integral for various aperture shapes to be

$$h_a / h_{eq} = \begin{cases} 1/2 & \text{circular aperture} \\ 0.55 & \text{square aperture} \\ 1 & \text{strip aperture} \end{cases} \tag{3.9}$$

where $h_{eq} = 2b_o$ is the equivalent height (spacing) of two parallel conductors. Furthermore, if the wires are of any arbitrary shape, then the result for an infinite aperture is

$$h_a / h_{eq} = 1/2 \tag{3.10}$$

Thus, the radiated field on boresight for the usual case of a circular aperture is

$$E_r(r, t) = \frac{V}{r} \frac{h_{eq}}{4\pi c f_g} \delta_a(r, t) \tag{3.10}$$

where the approximate delta function is defined in the previous section.

Note that the above contour integral was calculated with the assumption that the feed is long. This is an unnecessary constraint, as shown by Farr and Baum⁶, Appendix A. It is shown there that a reflection off a paraboloidal reflector produces a flat phase front with the same aperture field distribution as an infinitely long cylindrical transmission line (TEM mode), and is exactly expressed by the usual stereographic transformation (with minus sign, reflector transformation).

A SIMPLE MODEL OF THE IRA

In the previous section we described the impulsive portion of the radiation from the IRA on boresight. Now, we develop a simple expression for the entire waveform⁶.

Consider what happens when a step voltage drives the IRA shown in Figure 1. There is a prepulse for a time $2F/c$, where F is the focal length of the reflector. This is due to the direct radiation of the currents on the feed arms. The shape of this prepulse is a step function, similar to the driving voltage. In the last two sections we saw that the impulsive portion of the radiated field is an approximate delta function, so let us consider a radiated waveform shown in Figure 5. The area of the impulse is known from Sections 2 and 3. Furthermore, it is possible to calculate the direct radiation from a conical feed by using various stereographic projections. If the area under the prepulse is equal to the area under the impulse, then the tail portion of the waveform can be made small with proper tuning of the matching circuit.

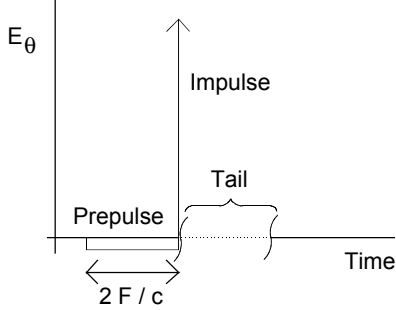


Figure 5. Step Response of an IRA.

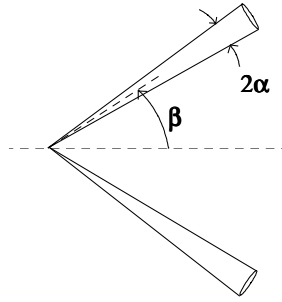


Figure 6. Circular cone IRA feed.

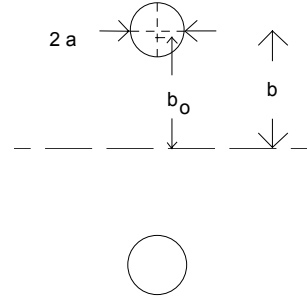


Figure 7. Projection of the conical feed onto a plane.

We calculate now the magnitude of the prepulse. It is simplest to calculate this for the geometry of two circular cones, as shown in Figure 6. If one were interested in a feed consisting of flat plates (either facing or coplanar), then for high impedances (small α) the results for the circular cones describe the plate geometries of angular width 4α as well. For lower impedances, more exact expressions are available⁶.

It is now necessary to project the spherical geometry of the circular cones onto a planar surface. In order to do so, we invoke the usual stereographic projection⁵. Thus, the polar coordinates in the projection plane are

$$x = 2F \cos(\phi) \tan(\theta/2), \quad y = 2F \sin(\phi) \tan(\theta/2) \quad (4.1)$$

The projection of the spherical cone generates a cylindrical structure whose cross-section is two circles with half height b and radius a such that

$$b = \frac{2F \sin(\beta)}{\cos(\alpha) + \cos(\beta)}, \quad a = \frac{2F \sin(\alpha)}{\cos(\alpha) + \cos(\beta)} \quad (4.2)$$

where a and b are as shown in Figure 7. It is simple to find the electric field at the center of the projected structure⁷. Thus, we find the backward radiated field (forward as far as our antenna is concerned) to be

$$E_{\theta} = -\frac{V}{r_o} \frac{\cos(\alpha) - \cos(\beta)}{\pi f_g \tanh(\pi f_g) \sin(\beta)} \quad (4.3)$$

This is just what we need for calculating the ratio of the prepulse area to the impulse area. The impulse area is found by integrating (3.10) with respect to time. The prepulse area is found by multiplying (4.3) by $2F/c$, the round trip transit time of the feed. The ratio of the prepulse area to the impulse area is found to be

$$\left| \frac{A_p}{A_i} \right| = \frac{4(F/D) [\cos(\alpha) - \cos(\beta)]}{\tanh(\pi f_g) \sin(\beta)} \quad (4.4)$$

If this ratio is approximately equal to unity, then the two areas are equal. A plot of the difference of this ratio from unity is shown in Figure 8. For the types of parameters in which one is typically interested ($F/D = 0.4$, $Z_{feed} = 400 \Omega$), the areas are equal to better than 1%. Thus, a reasonable expression for the on-boresight radiated field is

$$E(r, t) = \frac{V_o}{r} \frac{D}{4\pi f_g} \left[\frac{c}{2F} [-u(t) + u(t - 2F/c)] + \delta_a(t - 2F/c) \right] \quad (4.5)$$

Of course, this expression makes use of a number of assumptions, including the use of an ideal matching circuit at the boundary between the feed and reflector. A second assumption is that the aperture blockage is small (valid for thin feed projections). Nevertheless, it is very helpful that such a simple result is available for such a complex structure.

A number of design features are still to be considered in order to minimize the tail on the IRA. A design for the matching circuit is still under development. This design requires a calculation of the electric and magnetic moments of the IRA. Once these are known, the resistance of the matching circuit at low frequencies can be calculated, which will balance the two dipole moments. A second area of further work will

be to calculate the field scattered from the TEM feed and the reflector edges using diffraction theory. Both of these issues are currently being addressed.

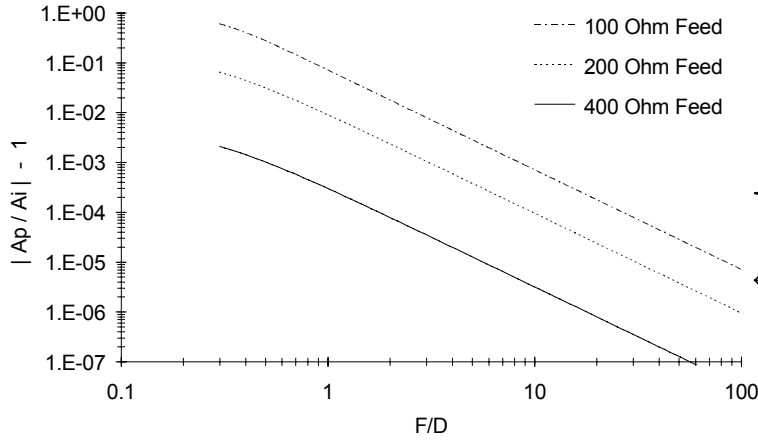


Figure 8. Error between the impulse area and prepulse area.

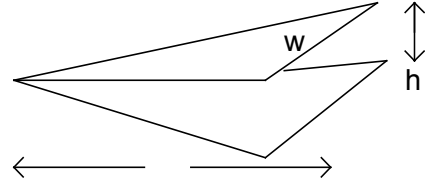


Figure 9. A TEM Horn.

TEM HORN

Another antenna sometimes used for radiating fast transients is the TEM horn (Figure 9). It is simplest to provide an analysis of a TEM horn by starting with the low frequencies. A low-frequency model of the TEM horn can be generated by using a simple open-circuit transmission-line model⁸. The model is generated by breaking the transmission line into a cascade of differential segments. The current and charge are known on each of these segments as a function of time, so they can be considered a cascade of small electric and magnetic dipoles. The fields radiated by each of these dipoles can be summed on boresight, leading to a low frequency model of

$$E(r, t) = -\frac{V_o}{r} \frac{h}{4\pi c f_g} \left[\delta_a(t) + \frac{c}{2} [-u(t) + u(t - 2/c)] \right] \quad (5.1)$$

where f_g is the ratio of the horn impedance to the impedance of free space, h is the height of the horn at its aperture, l is the length of the horn, and V_o is the magnitude of the voltage step launched onto the horn.

The above model is incorrect at high frequencies, because the early part of the step response is actually a step function. This is merely the $1/r$ extrapolation of the field at the aperture. In order to correct for this, it is necessary to flatten the top of the δ -function in the above equation, and broaden its width, while maintaining the same area⁸. The effective width (in seconds) of this flattened δ -function is just the area of the δ -function as determined by the low-frequency model, divided by the peak magnitude⁴. In the time domain, the step response has a form shown in Figure 10. This is roughly equivalent in the frequency domain to running the ideal step response through a low-pass filter of the form

$$G(\omega) = \frac{1}{1 + j\omega/\omega_2}, \quad \omega_2 = \frac{4\pi l c f_g}{h^2} \quad (5.2)$$

Although this filter function must be considered only approximate, it has been demonstrated that it has the correct mid-frequency and high-frequency behavior. The only ambiguity is its behavior near $\omega = \omega_2$.

The above results are valid only under the assumption of a matched load at the apex of the horn. If the source is not matched to the characteristic impedance of the horn, then there are multiple reflections within the TEM horn, and the above description is no longer valid. Furthermore, there is an assumption that there is no loss of signal as it passes through the matching circuit. This is therefore an idealized model, since normally there would be a factor of two loss in voltage as it passed through a matching circuit. Some suggestions for such matching networks are provided by Farr and Baum⁸.

There are a number of variations on the above rather simple design. In particular, one might consider using a lens in front of the TEM horn, in order to provide additional focusing⁹. This has the effect of sharpening the “broadened” delta function back to its original form. In doing so, this converts the antenna into a lens IRA⁸. Although this arrangement can considerably reduce the high-frequency rolloff of a TEM horn, it should be pointed out that lenses can be very heavy.

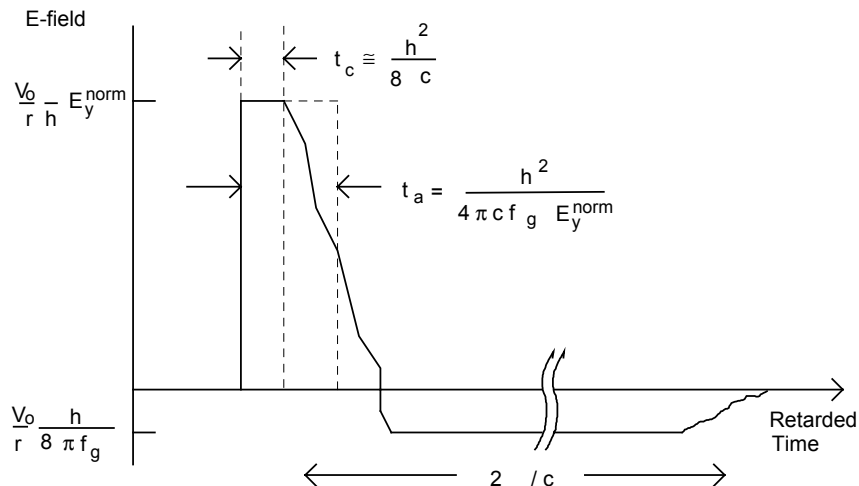


Figure 10. Step Response of a TEM horn.

AN EXAMPLE: TEM HORN AND TWO SIZES OF IRA

We compare now the performance of a TEM horn to two IRAs. One IRA (medium size) has a diameter equal to the length of the TEM horn, while the other IRA (small size) has the same aperture area as the TEM horn, as shown in Figure 11. The TEM horn has an impedance of $\sim 116 \Omega$, while both IRA's have feed impedances of 400Ω and F/D ratios of 0.4. The TEM horn is driven with 200 kV peak voltage, while the IRA's are driven with 371 kV, providing the same power to both antennas. Note that various baluns are required for both cases, which may require conversion of single-ended signal to differential. The driving voltage is a double exponential with a 200 ps. 10-90% risetime and a long decay time.

The frequency domain step response of the three antennas at 1 km on boresight is shown in Figure 12. The response to the driving voltage at 1 km is shown in the time domain in Figure 13. The response of both IRAs is better than that of the TEM horn everywhere except at very low frequencies for the small IRA. The high-frequency rolloff of the TEM horn is clear from these results.

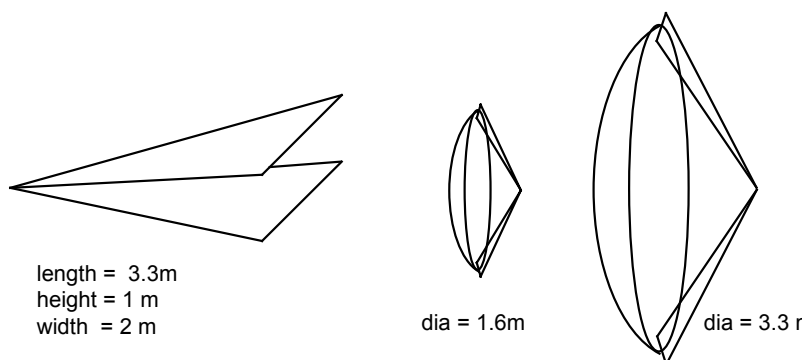


Figure 11. TEM horn and two sizes of IRA for comparison. The center IRA (small) has the same aperture area as the TEM horn, while the right IRA (medium) has a diameter equal to the length of the TEM horn.

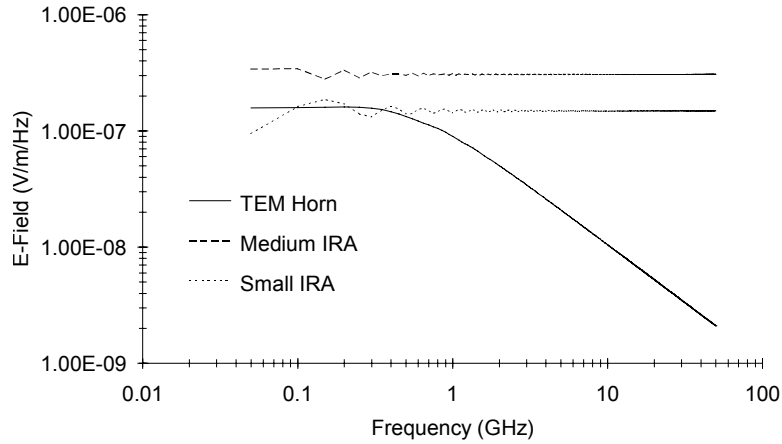


Figure 12. Step responses of the TEM horn and two IRA's at 1 km.

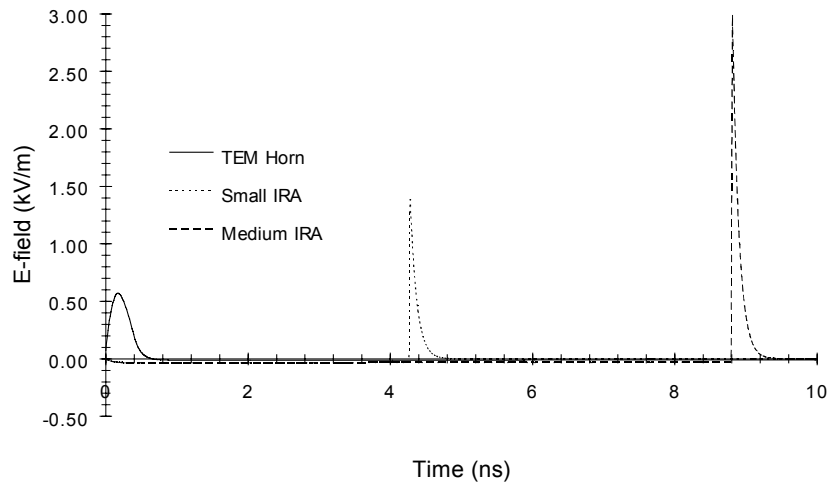


Figure 13. Time domain response of the three antennas at 1 km.

CONCLUSION

We have described in detail the behavior of Impulse Radiating Antennas in a number of different ways. In addition, we have compared the response of IRAs to TEM horns. We find that IRAs are best for radiating fast risetime pulses because their step response does not roll off at the high end.

It is appropriate to note a number of caveats in the analysis presented here. We have assumed an ideal matching circuit in the IRA, as well as an idealized feed circuit in the TEM horn. We have made no attempt to design the matching circuits or baluns, (although some ideas on baluns for IRAs are provided by Baum¹⁰). Furthermore, the high-voltage properties of the two antennas have been ignored. Nevertheless, we can draw some important conclusions from the above data. The data suggest that an IRA is a promising antenna for radiating fast transient pulses. When comparing antennas of similar size (largest dimension), the IRA has a considerable advantage in performance. When comparing antennas of similar aperture area, the IRA still has clear advantages at the high end, since it does not suffer the high-frequency rolloff problem of the TEM horn. Finally, the IRA has some desirable directionality at low frequencies.

REFERENCES

1. E. G. Farr and J. S. Hofstra, An Incident Field Sensor for EMP Measurements, Sensor and Simulation Note 319, November 6 1989.
2. C. E. Baum, General Properties of Antennas, Sensor and Simulation Note 330, July 23 1991.
3. C. E. Baum, Radiation of Impulse-Like Transient Fields, Sensor and Simulation Note 321, November 25 1989.
4. C. E. Baum, Aperture Efficiencies for IRAs, Sensor and Simulation Note 328, June 24 1991, and 1992 APS/URSI/NEM Symposium Proceedings, July 20-24, 1992, Chicago.
5. W. R. Smythe, *Static and Dynamic Electricity*, Third Ed., Hemisphere, 1989, p. 76 and p. 460.
6. E. G. Farr and C. E. Baum, Prepulse Associated with the TEM Feed of an Impulse Radiating Antenna, Sensor and Simulation Note 337, March 1992.
7. C. E. Baum, Impedances and Field Distributions for Symmetrical Two Wire and Four Wire Transmission Line Simulators, Sensor and Simulation Note 27, October 10 1966.
8. E. G. Farr and C. E. Baum, A Simple Model of Small-Angle TEM horns, Sensor and Simulation Note 340, May 1992.
9. C. E. Baum and A. P. Stone, *Transient Lens Synthesis*, Hemisphere, 1991.
10. C. E. Baum, Configurations of TEM Feed for an IRA, Sensor and Simulation Note 327, April 27, 1991.